

# ACYL CHAIN ORIENTATIONAL ORDER IN THE HEXAGONAL $H_{II}$ PHASE OF PHOSPHOLIPID-WATER DISPERSIONS

EDWARD STERNIN,\* BERNARD FINE,\* MYER BLOOM,\* COLIN P. S. TILCOCK,† KIM F. WONG,‡  
AND PIETER R. CULLIS‡

\*Department of Physics and †Department of Biochemistry, The University of British Columbia

**ABSTRACT** The deuterium nuclear magnetic resonance ( $^2\text{H}$  NMR) spectrum of perdeuterated tetradecanol in a mixture of 1-palmitoyl-2-oleoyl-phosphatidylethanolamine (POPE) and water was used to compare the variation of the acyl chain orientational order parameter,  $S(n)$ , with carbon position,  $n$ , in the liquid crystalline lamellar ( $L_\alpha$ ) and hexagonal ( $H_{II}$ ) phases. The characteristic independence of  $S(n)$  with  $n$  (plateau) normally observed in the  $L_\alpha$  phase is replaced by a more rapid decrease of  $S(n)$  with  $n$  in the  $H_{II}$  phase. It is suggested that as a consequence of the geometrical characteristics of the  $H_{II}$  phase, there is an increase in conformational freedom available to different parts of the acyl chain.

## INTRODUCTION

The technique of deuterium nuclear magnetic resonance ( $^2\text{H}$  NMR) has provided microscopic information on local orientational order of the acyl chains in phospholipid bilayer model membranes (Mantsch et al., 1977; Seelig and Seelig, 1980; Davis, 1983) and in biological membranes under physiologically relevant conditions (Seelig, 1977; Seelig and Seelig, 1980; Jacobs and Oldfield, 1981; Devaux, 1983; Bloom and Smith, 1985). Measurements of  $S(n)$  in biological membranes have also yielded important information on lipid-protein interactions (Seelig and Seelig, 1980; Devaux, 1983; Bloom and Smith, 1985; Mouritsen and Bloom, 1985).

The orientational order parameter associated with the  $n$ th carbon atom on an acyl chain is given by the ensemble average

$$S(n) = \frac{1}{2}(3 \cos^2 \theta_n - 1), \quad (1)$$

where  $\theta_n$  is the angle between the  $n$ th C-D bond and the axis of symmetry for rapid motions of the acyl chain. For the lamellar liquid crystalline ( $L_\alpha$ ) phase, structural measurements of model membranes made using the traditional diffraction techniques can only provide a measure of a single parameter, which can be the surface area per molecule or, equivalently for an incompressible fluid, membrane bilayer thickness (Janiac et al., 1976; Lis et al., 1982; Cornell and Separovic, 1983; Lewis and Engelman, 1983). Measurements of  $S(n)$  are thus an important complementary source of structural and dynamical information in model membranes.

The fluid bilayer signature (Seelig and Seelig, 1980) of  $S$  versus  $n$  is characterized by a plateau (*i.e.*, very little

variation of  $S$  with  $n$ ) for the part of the acyl chain closer to the glycerol backbone, followed by a relatively rapid decrease towards the end of the chain (Seelig, 1977; Seelig and Seelig, 1980). This behavior can be understood in terms of models which take account of the following features of lipid bilayers (Seelig, 1977; Jähnig, 1979; Seelig and Seelig, 1980; Dill and Flory, 1980): (a) the lamellar symmetry of the phospholipid bilayers and the amphiphilic nature of the phospholipid molecules; (b) rapid axial rotation about the bilayer normal in the  $L_\alpha$  phase and also rapid conformational averaging of the NMR observables associated with deuterons on the acyl chains; (c) the existence of an effective molecular field parallel to the bilayer normal due to interactions between neighboring phospholipid molecules.

The variation of the orientational order parameter with chain position can also be studied in the hexagonal ( $H_{II}$ ) phase of a phospholipid-water dispersions. In this phase, the water is found on the inside of long parallel cylinders which are hexagonally coordinated in the plane perpendicular to their axes of symmetry as shown schematically in Fig. 1. The hydrophobic acyl chains fill the space between the cylinders. It is well established from phosphorus ( $^{31}\text{P}$ ) NMR measurements (Cullis and de Kruijff, 1979) that the lipid molecules diffuse rapidly around the cylinder axes on the NMR time scale. This feature, the symmetry properties of the  $H_{II}$  phase, and in particular, the anticipated nature of the acyl chain packing in the regions between the cylinders led us to expect a qualitatively different dependence of orientational order on chain position. This expectation is supported by measurements made by Jarrell and coworkers (1986; also Perly et al., 1985) which give the changes in orientational order between  $L_\alpha$  and  $H_{II}$  phases

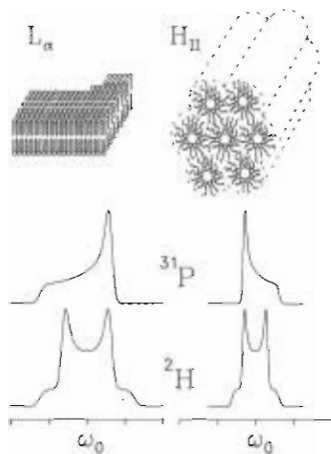


FIGURE 1 Comparison of the  $L_{\alpha}$  (left) and hexagonal  $H_{II}$  (right) phases of phospholipid-water dispersions. A schematic representation of their geometry is shown at the top. Due to the rapid diffusion around the cylinder axes in the  $H_{II}$  phase, both the  $^{31}\text{P}$  NMR (middle) and the  $^2\text{H}$  NMR (bottom) spectra are scaled by a factor of  $-1/2$ . The  $^{31}\text{P}$  NMR spectra can yield both the absolute value of  $S$  and its sign. Because of their symmetry, the  $^2\text{H}$  NMR spectra do not provide the information about the sign of  $S$ . For illustrative purposes, the simulated powder patterns are

shown on arbitrary horizontal and vertical scales, with  $\omega_0$  indicating the Larmor frequency for each nucleus.

for some selected chain positions. Here, we present the first systematic study of the variation of  $S$  with  $n$ , which enables us to analyze quantitatively differences in chain packing between the  $L_{\alpha}$  and  $H_{II}$  phases. As we shall see, substantial differences are indeed observed. We present our experimental results in the hope that they stimulate theoretical studies of the differences in local orientational order between  $H_{II}$  and  $L_{\alpha}$  phases in relation to their symmetry properties.

## MATERIALS AND METHODS

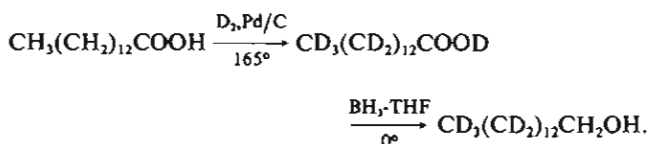
The  $^2\text{H}$  NMR and  $^{31}\text{P}$  NMR measurements to be described below were carried out in ternary alcohol-lipid-water mixtures. The alcohol used was tetradecanol (TD) deuterated in carbon positions 2–14. Lipids having phosphatidylcholine (PC) and phosphatidylethanolamine (PE) headgroups were used and the two chains were either two oleoyl chains (DOPC or DOPE) or 1-palmitoyl-2-oleoyl (POPC or POPE).

### Materials

1-palmitoyl-2-oleoyl-phosphatidylethanolamine (POPE) and 1-palmitoyl-2-oleoyl-phosphatidylcholine (POPC) were purchased from Avanti Polar Lipids, Inc., (Birmingham, AL). Deuterium depleted water ( $0.0033 \times$  natural abundance) and borane-tetrahydrofuran complex (1.0 M solution in tetrahydrofuran) were purchased from Aldrich Chemical Co., Milwaukee, WI.  $\text{D}_2\text{O}$  (99.8 atom percent purity) was supplied by Merck Frost Canada Inc., Montreal, PQ. Tetradecanoic acid was purchased from Sigma Chemical Co., St. Louis, MO. Palladium on charcoal (9% Pd) was obtained from VWR Scientific Div., Univar, San Francisco, CA.

### Synthesis of Perdeuterated Tetradecanol

Perdeuterated tetradecanol was prepared from tetradecanoic acid as outlined in the following equation:



Perdeuterated tetradecanoic acid was prepared by hydrogen/deuterium exchange between the fatty acid (five parts) and deuterium gas at atmospheric pressure over 9% palladium on charcoal (one part) catalyst at  $165^\circ\text{C}$  (Hsiao et al., 1974; Delikatny, 1987). The deuteration process, stopped at 80%, was monitored periodically by mass spectroscopy carried out with a Kratos MS50 mass spectrometer. The perdeuterated tetradecanoic acid, purified by column chromatography (silica gel 60–120 mesh) and recrystallized from methanol (melting point  $57\text{--}58^\circ\text{C}$ ), was reduced to the corresponding alcohol by borane in tetrahydrofuran (THF) at  $0^\circ\text{C}$  (Yoon et al., 1973). The tetradecanol so obtained was redistilled under vacuum (boiling point  $100\text{--}102^\circ\text{C}$  at 0.5 mm Hg). It has a melting point of  $39\text{--}40^\circ\text{C}$  when recrystallized from aqueous ethanol. Due to the nature of the synthetic procedure, only carbon positions 2–14 of the tetradecanol are deuterated.

## Sample Preparation

Stock solutions of POPE and POPC in chloroform were made and phosphate assays were done to determine their lipid concentration. A 0.1 M solution of the perdeuterated tetradecanol was also prepared. An amount of lipid stock solution containing 200  $\mu\text{M}$  of lipid was placed in a test tube and mixed with the required amount of tetradecanol solution. The chloroform was evaporated off, first under nitrogen and subsequently, under reduced pressure for at least 2 h. Once dry, the sample was dissolved in a small amount of cyclohexane and transferred to glass NMR sample holders, 8 mm in diameter and 17 mm long. These were placed in a  $-80^\circ\text{C}$  freezer for 1 h and then immediately transferred to a vacuum and left there overnight. An excess of buffer composed of 20 mM HEPES and 300 mM NaCl in deuterium depleted water at pH 7.4 was added and then the sample was sealed with a teflon plug.

### $^{31}\text{P}$ NMR

$^{31}\text{P}$  NMR spectra were obtained on a WP200 FT-NMR spectrometer (Bruker Instruments, Inc., Billerica, MA). The lipid sample, in a sealed sample holder, was placed in a 10-mm round bottom NMR tube and the sample holder was then completely covered with  $^2\text{H}_2\text{O}$  to provide the locking signal. The spectrometer was operated at 81 MHz with broadband proton decoupling of 10 W. The spectra were collected for at least 500 transients with a 20 kHz sweep width, an 18  $\mu\text{s}$   $90^\circ$  pulse and a repetition rate of  $1\text{s}^{-1}$ . Temperature was maintained by a Bruker B-VT 1000 temperature controller to  $\pm 0.5^\circ\text{C}$ . Ten minutes were allowed for the sample to equilibrate at each temperature. Since hysteresis has been observed in the  $L_{\alpha}$  to  $H_{II}$  phase transition, spectra were always collected first at the lowest temperature and then at increasingly higher temperatures. Samples were stored at  $-20^\circ\text{C}$  overnight before collecting spectra at a lower temperature.

### $^2\text{H}$ NMR

Deuterium NMR spectra were obtained on a home-built 35 MHz  $^2\text{H}$  NMR spectrometer described in detail elsewhere (Davis, 1979; Sternin, 1985). Spectra were collected for at least 20,000 transients each using a quadrupolar echo pulse sequence and phase cycling (Davis, 1979; Davis, 1983; Rance and Byrd, 1983). The  $90^\circ$  pulse length was 2.5–3.5  $\mu\text{s}$  and repetition rate was  $2\text{s}^{-1}$ . The time between the two pulses in the quadrupolar pulse sequence was 50  $\mu\text{s}$ . Spectra consisted of 2,048 complex data points each and the dwell time varied from 1 to 5  $\mu\text{s}$ . A modified Bruker B-ST 100/700 temperature controller was used to maintain the temperature of an oven enclosing the sample and the radio frequency coil to within  $\pm 0.1^\circ\text{C}$ . The absolute temperature calibration was  $\pm 1^\circ\text{C}$ . The sample was allowed at least 30 min to equilibrate at each temperature. To avoid hysteresis effects spectra were always collected at increasing temperatures, as described for the  $^{31}\text{P}$  NMR spectra.

### DePakeing

The obtained spectra exhibit the powder pattern lineshape characteristic of superposition of randomly oriented domains. An effective way of

analyzing such powder spectra quantitatively is provided by the numerical dePakeing procedure (Bloom et al., 1981; Sternin et al., 1983). The dePakeing procedure converts a powder spectrum into one characteristic of an oriented bilayer or cylinder, and thus provides the actual distribution of values of  $S(n)$ .

## RESULTS

The  $^{31}\text{P}$  NMR spectra obtained with 20 mol% TD in POPE at temperatures varying from 26° to 56°C are shown in Fig. 2. These spectra indicate that the  $L_\alpha$  to  $H_{II}$  transition occurs between 36° and 46°C. This is ~15° lower than in pure POPE. As expected (Tilcock et al., 1986),  $^{31}\text{P}$  NMR spectra (not shown) of POPC with 20 mol% TD over the same range of temperatures showed that the sample remained in the  $L_\alpha$  phase.

The  $^2\text{H}$  NMR spectra of 20 mol% TD in POPE at varying temperatures are shown in Fig. 3. Below the  $L_\alpha$  to  $H_{II}$  transition (as determined from the  $^{31}\text{P}$  NMR) the  $^2\text{H}$  NMR spectra exhibit the usual lamellar lineshape for a perdeuterated chain (Davis, 1979; Thewalt et al., 1985). Above the transition the lineshape is significantly different. In the immediate vicinity of the transition, spectra containing mixtures of both lineshapes are obtained. By contrast, the  $^2\text{H}$  NMR spectrum (not shown) of 20 mol% TD in POPC exhibits a characteristic lamellar lineshape over the same temperature range, with a gradual reduction in its overall width as the temperature is increased.

## DISCUSSION

Molecules in the  $H_{II}$  phase diffuse rapidly about the cylinder axes on the NMR time scale. If this were the only difference between  $L_\alpha$  and  $H_{II}$  phases then for a nucleus near the lipid-water interface, the effective symmetry axis for the spin-dependent interactions would be rotated by

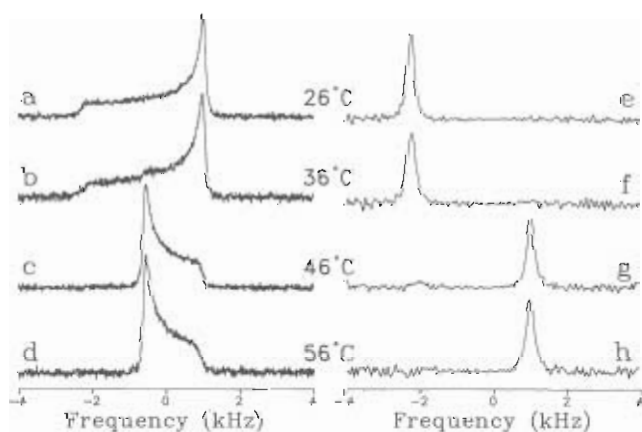


FIGURE 2  $L_\alpha$  to  $H_{II}$  phase transition as seen from the  $^{31}\text{P}$  NMR spectra. The results of dePakeing the powder spectra on the left (a-d) are shown on the right (e-h) for four different temperatures. The phase transition occurs between 36° and 46°C. By convention, the depaked spectra are shown for the orientation corresponding to  $\theta = 0$  (shoulder), and the position of the depaked peak gives both the sign and the absolute value of  $S$ . Note the small remnant of the  $L_\alpha$  phase in the depaked spectrum of g, almost impossible to see in the powder spectrum of c. Binomial smoothing over  $\pm 3$  points was used on the depaked spectra.

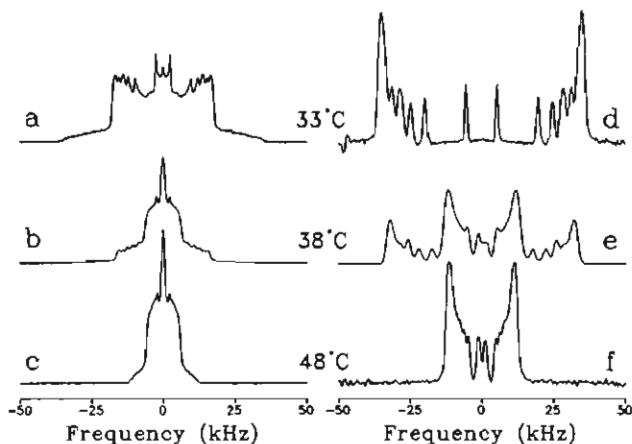


FIGURE 3  $L_\alpha$  to  $H_{II}$  phase transition as seen from the  $^2\text{H}$  NMR spectra. The results of dePakeing the powder spectra on the left (a-c) are shown on the right (d-f) for three different temperatures. The spectrum in a (and in d) exhibits the plateau lineshape characteristic of the  $L_\alpha$  phase; the lineshape of c (and of f) is completely different. In the immediate vicinity of the phase transition (b and e) a mixture of both lineshapes is observed. The integral intensity of all spectra is normalized to 1, but for clarity the spectrum in a is shown at twice the vertical scale of those in b and c. By convention, the depaked spectra are shown for the orientation corresponding to  $\theta = 0$  (shoulder). Binomial smoothing over  $\pm 3$  points was used on the depaked spectra.

90°, from the normal to the lipid-water interface to the direction of the cylinder axis. From Eq. 1 it may be seen that this gives rise to a change in  $S$  by a factor of  $-1/2$ . Because of their symmetry,  $^2\text{H}$  NMR spectra are sensitive only to the magnitude of  $S$  and not to its sign. However,  $^{31}\text{P}$  NMR spectra manifest both the factor of  $1/2$  (actually, 0.46–0.47 as measured from the depaked spectra) and the sign change. This may be seen from a comparison of the  $^{31}\text{P}$  NMR spectra of the  $L_\alpha$  phase with those of the  $H_{II}$  phase in Fig. 2.

Here we investigated via  $^2\text{H}$  NMR the orientational order of the acyl chain of perdeuterated TD in the lipid-water mixtures. In a sense, the TD molecule was used as a reporter of the orientational order along the chains of the lipid molecules. In fact, adding alcohol to the lipid-water mixtures has a strong effect on the temperature of the phase transition. This suggests that such systems should really be treated as ternary. Nevertheless, since TD does have a polar end, we expect it to be pinned down to some extent at the lipid-water interface with its acyl chain extending into the bulk of the lipid, and therefore, to be a good reporter of the orientational order of the acyl chains of the host lipid. This has been confirmed in a recent study of alcohol-lipid-water mixtures in the  $L_\alpha$  phase (Thewalt et al., 1986).

Inspection of the  $^2\text{H}$  NMR spectra of perdeuterated TD in POPE in Fig. 2 shows that the lineshapes in the  $L_\alpha$  and  $H_{II}$  phases are different from each other. This indicates that across the phase transition the various  $S(n)$  values along the TD chain do not scale by a common factor. Also, measuring the average quadrupolar splitting as a function

of temperature gives a decrease by considerably more than a factor of two. These two observations agree with our expectations since the geometry of the  $H_{II}$  phase allows more conformational freedom for the ends of the chains than that of the  $L_\alpha$  phase.

An important and much discussed feature of the variation of  $|S(n)|$  in the  $L_\alpha$  phase is the plateau. In the depaked spectrum of the  $L_\alpha$  phase shown in Fig. 3 *d*, the plateau corresponds to the largest splitting, which accounts for almost half of the total intensity. In the  $H_{II}$  phase, shown in Fig. 3 *f*, a relatively larger fraction of the total intensity appears at smaller splittings, indicating a diminishing importance of the plateau. This point is more readily seen from the renormalized plots of Fig. 3 *d* and *f* shown in Fig. 4. Here we plot the spectral intensity against the variable  $\sigma = S/S_{\max}$ , where  $S_{\max}$  is the maximum value of the local chain orientational order parameter in a given phase, as measured from the maximum observed splittings in Fig. 3 *d* and *f*. In addition, the area of each spectrum has been normalized to 27, the number of  $^2\text{H}$  nuclei per TD chain contributing to the  $^2\text{H}$  NMR spectra. This corresponds to twelve methylene (position one is not deuterated) and one methyl group. Therefore, each curve can be viewed as a plot of the number of deuterons per unit interval of  $\sigma$ . The plots show clearly that the  $H_{II}$  phase no longer has a plateau near  $\sigma = 1$  and that the distribution of  $\sigma$  is more heavily weighted at lower values in the  $H_{II}$  phase relative to the  $L_\alpha$  phase.

If one now assumes that  $\sigma$  varies monotonically along the

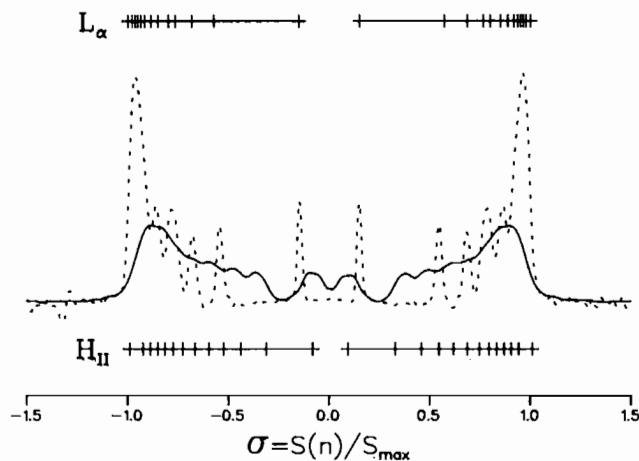


FIGURE 4 Comparison of the distribution of the fractional order parameter in the two phases.  $L_\alpha$  phase, shown by the dotted line, exhibits the characteristic plateau lineshape where a major fraction of the total intensity is in the outermost peaks of the spectrum. In contrast, in the  $H_{II}$  phase, shown by the solid line, the importance of the plateau is diminished. Both spectra are normalized to have the total intensity of 27. The fractional order parameter for every carbon position is assigned by calculating the midpoints of intervals weighted 3-2-2-2-..., as discussed in text. Their locations are shown for both phases, immediately above (for  $L_\alpha$ ) and the below (for  $H_{II}$ ) the spectra. Notice, that the tick marks corresponding to these midpoints are more evenly spaced for the  $H_{II}$  phase.

chain, one can assign an average fractional order parameter in each phase to every carbon position  $n$ . This is denoted by  $\sigma_L(n)$  for the  $L_\alpha$  phase and  $\sigma_H(n)$  for the  $H_{II}$  phase. In practice, we separately assign the peaks associated with the smallest values of  $\sigma$  in Fig. 4 to the methyl deuterons. The remaining area under the curve corresponds to 24 deuterons and is divided into 12 equal parts. The value of  $\sigma$  at the center of each of these parts determines the value of  $\sigma_L(n)$  or  $\sigma_H(n)$  corresponding to the appropriate methylene group in the chain. The plots of the average  $\sigma(n)$  values for each phase assigned in this manner are shown in Fig. 5.

A more appropriate way of characterizing the systematic differences in conformational averaging along the chain is by the ratio

$$R(n) = \frac{\sigma_H(n)}{\sigma_L(n)}. \quad (2)$$

This ratio should in principle be determined from spectra obtained at a common temperature, such as in Fig. 3 *e*. Since we are unable to separate the coexisting spectra in Fig. 3 *e*, we calculate the values of  $R(n)$  under the assumption that the  $L_\alpha$  and  $H_{II}$  spectra approximately scale with temperature, *i.e.*, that  $S_H(n)/(S_H)_{\max}$  and  $S_L(n)/(S_L)_{\max}$  do not change appreciably for a small change in temperature. Therefore, we approximate  $R(n)$  by the ratio  $\sigma'_H(n)/\sigma'_L(n)$ , where  $\sigma'_H$  and  $\sigma'_L$  are measured from the spectra of pure  $H_{II}$  and  $L_\alpha$  phases in Fig. 4 *f* and *d*, respectively. The resulting  $R(n)$  versus  $n$  is plot is presented in Fig. 6. Note that this approximation is only valid for the dimensionless quantity  $\sigma$ . If we measure the ratio of maximum quadrupolar splittings in the same way, we obtain  $(S_H)_{\max}/(S_L)_{\max} = 12.94/36.28 \approx 1/2.8$ . On the

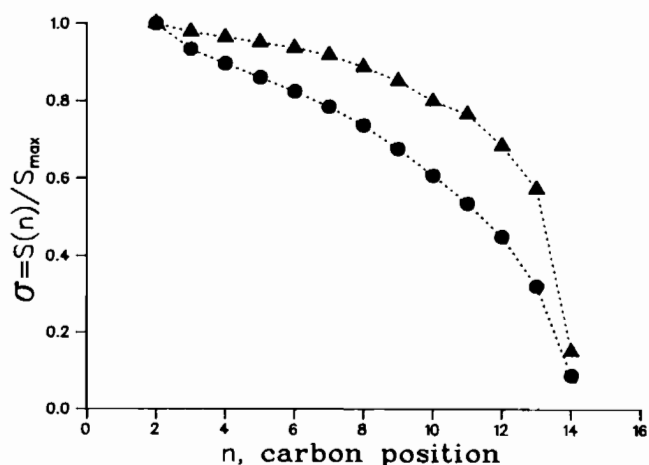


FIGURE 5 Order parameter profile of  $L_\alpha$  ( $\blacktriangle$ ) and  $H_{II}$  ( $\bullet$ ). We use the assumption that  $\sigma$  decreases monotonically with carbon position to divide the integrated intensity, normalized to 27, into the intervals of weight 3-2-2-2-..., and assign the midpoints of these intervals to the average fractional order parameter associated with the appropriate carbon position. In this way,  $S_{\max}$  in each phase is the one associated with the outermost such interval which we assign to the carbon position  $n = 2$ . Consequently,  $\sigma_L(2) = \sigma_H(2) = 1$ .

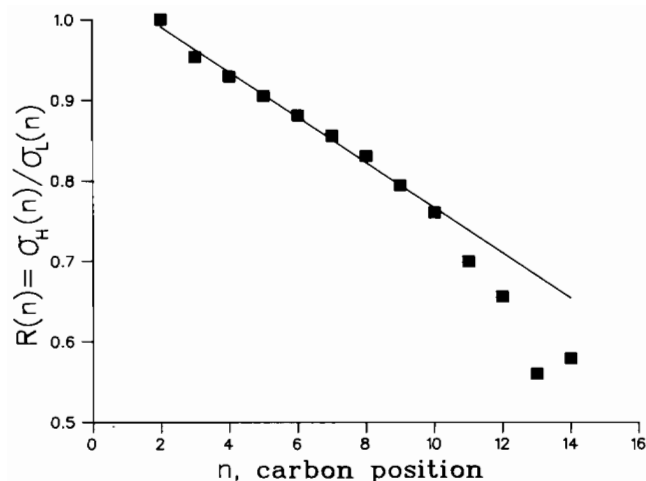


FIGURE 6 Ratio of the fractional order parameters,  $\sigma(n)$ , in the  $L_\alpha$  and  $H_{II}$  phases. The increase of the orientational freedom available to the acyl chain in the  $H_{II}$  phase is approximately linear as compared with the  $L_\alpha$  phase. The straight line is the result of a linear least squares fit to the first nine points (carbon positions  $n = 2$  to  $n = 10$ ).

other hand, measuring the same ratio from the coexisting spectra of Fig. 3 *e*, yields  $(S_H)_{\max}/(S_L)_{\max} \approx 1/2.4$ .

The almost linear decrease of  $R(n)$  with  $n$  provides a measure of the increase in conformational freedom available for different parts of the TD chain when the system undergoes the  $L_\alpha$  to  $H_{II}$  phase transition. Note that the ratio of the maximum splittings, which we associate with  $n = 2$ , differs from  $1/2$ . This is probably indicative of the degree to which the polar end of the TD molecule is pinned down to the lipid-water interface.

#### CONCLUDING REMARKS

Most previous NMR studies of phospholipid  $H_{II}$  phases have been carried out using  $^{31}\text{P}$  NMR (Cullis and de Kruijff, 1979). In agreement with these studies, our  $^{31}\text{P}$  NMR measurements show that the ratio of the  $^{31}\text{P}$  anisotropic chemical shift in the  $H_{II}$  phase to that in the  $L_\alpha$  phase is  $\sim -1/2$ . This result demonstrates that the conformational averaging of the polar headgroup region of the phospholipid molecules is not appreciably affected by the curvature of the cylindrical lipid-water interface in the  $H_{II}$  phase. Equivalently, one can say that the local orientational order parameter for the polar headgroup is not affected by this curvature. The factor of  $-1/2$  is attributable to the rapid diffusive motion of the lipid molecules around the cylinder axes. By contrast, we have shown that the local orientational order of the acyl chains, as sensed by  $^2\text{H}$  NMR of the TD molecules in our samples, is systematically lower in the  $H_{II}$  phase than in the  $L_\alpha$  phase. For the  $n = 2$  position, the ratio of the quadrupolar splittings in the  $H_{II}$  phase to that of the  $L_\alpha$  phase is  $1/2.4$ ; near the end of the chain this ratio decreases to  $\sim 1/5.0$ . The fact that the ratio of  $1/2.4$  is within 20% of the factor  $-1/2$  demonstrates that the polar end of the TD molecule spends most of its time close to the

lipid-water interface, while the systematic additional decrease of  $S_H(n)$  down the chain indicates significantly greater angular freedom deep in the hydrophobic region of the  $H_{II}$  phase as compared with the  $L_\alpha$  phase.

The theoretical methods required to interpret the dependence of  $S$  on  $n$  in amphiphilic systems of various geometries are now well established (Jähnig, 1979; Dill and Flory, 1980; Seelig and Seelig, 1980; Ben-Shaul and Gelbart, 1985) but have not, to our knowledge, been applied to the geometry of the  $H_{II}$  phase. We hope that our work will stimulate such calculations. An explicit prediction that a system with a cylindrical lipid-water interface should exhibit a more rapid decrease of  $S$  with  $n$  than that of a planar interface was made by de Gennes (1974). This qualitatively agrees with our experimental observations. On the other hand, studies of  $S$  versus  $n$  for the hexagonal  $H_I$  phase of a soap-water system (Mely et al., 1975) were in disagreement with de Gennes' prediction. The  $H_I$  phase is the reverse of the  $H_{II}$  phase in the sense that the water in the  $H_I$  phase is outside the cylinders and the chains are inside. Theoretical studies of the type we propose above should account for the different properties of the  $H_I$  and  $H_{II}$  phases.

Our analysis of  $S$  versus  $n$  was carried out using experimental  $^2\text{H}$  NMR spectra of perdeuterated rather than specifically labeled chains. This resulted in an enormous saving of time and money since one sample sufficed for the entire  $S(n)$  profile. We used the dePakeing method to establish a correct probability distribution for  $S$ . Its reliability for perdeuterated chains is by now well established (Bloom et al., 1981; Davis, 1983; Pauls et al., 1983; Sternin et al., 1983). However, our analysis was based on the assumption that  $S$  varies monotonically with  $n$ . This assumption is, in fact, not rigorously correct. It is well known that there is a small oscillation in  $S(n)$  between odd and even values of  $n$  because of the geometry of the acyl chain (Seelig and Seelig, 1980; page 36). Our results should be compared with the orientational order of a smooth curve drawn through the mid-points of the C-C bonds, much in the spirit of representing the chains by continuous elastic lines (Jähnig, 1979). We feel strongly, however, that in most cases the crucial physical information provided by  $^2\text{H}$  NMR measurements is associated with the properties of this smooth curve.

Finally, we wish to comment on future prospects for measurements of the type reported here. Here, TD molecules were used to probe the orientational order of the host lipid in the  $L_\alpha$  and  $H_{II}$  phases. In the case of  $L_\alpha$  phase, previous studies have shown that molecules such as TD (Thewalt et al., 1985; Thewalt et al., 1986) and fatty acids (Pauls et al., 1983) do perturb the orientational order of the host phospholipid molecules, but that they report accurately on this perturbed orientational order. It would be desirable to compare the  $S(n)$  profile for the acyl chains of the phospholipid molecules in the  $H_{II}$  phase with those

reported here for TD, and we plan to do so. Another aspect of the problem, and the one which originally attracted us to these systems, is the great influence that a small amount of alcohol has over the phase behavior of the lipid-water dispersions, effectively facilitating the transition to the  $H_{II}$  phase. Our data seems to imply that the alcohol molecules are pinned down to a certain degree at the lipid-water interface. Thus it will be of interest to examine the partition of TD and phospholipid molecules in the various regions of the  $H_{II}$  phase. One way to do this would be to replace TD by an appropriate perdeuterated alkane, which does not have a polar end and may therefore preferentially migrate deeper into the hydrophobic region of the  $H_{II}$  phase. This may preferentially affect the orientational order of the ends of the acyl chains of the phospholipid, as the alkane would fill up the pockets in the middle of the triangles formed by the nearest-neighbor cylinders of the  $H_{II}$  phase (Kirk and Gruner, 1985).

We would like to thank Dr. E. J. Delikatny for his help with the synthesis of the deuterated TD. We are indebted to Drs. J. L. Thewalt and S. M. Gruner for helpful discussions. The figures in this paper were prepared using the computer graphics software developed at The University of Meson Facility, Vancouver, BC).

The financial support of the Natural Sciences and Engineering Research Council (NSERC) and the Medical Research Council (MRC) of Canada is gratefully acknowledged. Pieter R. Cullis is an MRC scientist.

Received for publication 4 February 1988 and in final form 6 June 1988.

## REFERENCES

Ben-Shaul, A., and W. M. Gelbart. 1985. Theory of chain packing in amphiphilic aggregates. *Annu. Rev. Phys. Chem.* 36:179-211.

Bloom, M., J. H. Davis, and A. L. MacKay. 1981. Direct determination of the oriented sample NMR spectrum from the powder spectrum for systems with local axial symmetry. *Chem. Phys. Lett.* 80:198-202.

Bloom, M., and I. C. P. Smith. 1985. Manifestations of lipid-protein interactions in deuterium NMR. In *Progress in Protein-Lipid Interactions*. A. Watts and J. J. H. M. DePont, editors. 61-88. Elsevier North-Holland Biomedical Press, Amsterdam.

Cornell, B. A., and F. Separovic. 1983. Membrane thickness and acyl chain length. *Biochim. Biophys. Acta.* 733:189-193.

Cullis, P. R., and B. de Kruijff. 1979. Lipid polymorphism and the functional roles of lipids in biological membranes. *Biochim. Biophys. Acta.* 559:399-420.

Davis, J. H. 1983. The description of lipid membrane conformation, order, and dynamics by  $^2\text{H}$  NMR. *Biochim. Biophys. Acta.* 737:117-171.

Davis, J. H. 1979. Deuterium magnetic resonance study of the gel and liquid crystalline phases of dipalmitoylphosphatidylcholine. *Biophys. J.* 27:339-358.

de Gennes, P. G. 1974. General features of lipid organization. *Phys. Lett.* 47A:123-124.

Delikatny, E. J. 1987. NMR Studies of Carboxylic Acids: An Investigation of Head Group Behaviour in Lyotropic and Nematic Phases. Ph.D. thesis, University of British Columbia, Vancouver, BC, 67-70.

Devaux, P. F. 1983. ESR and NMR studies of lipid-protein interactions in membranes. In *Biological Magnetic Resonance*. L. J. Berliner and J. Reuben, editors. 183-299. Plenum Publishing Co., New York.

Dill, K. A., and P. J. Flory. 1980. Interphases of chain molecules:

monolayers and lipid bilayer membranes. *Proc. Natl. Acad. Sci. USA.* 77:3115-3119.

Hsiao, C. Y. Y., C. A. Ottaway, and D. B. Wetlaufer. 1974. Preparation of fully deuterated fatty acids by simple method. *Lipids.* 9:913-915.

Jacobs, R. E., and E. Oldfield. 1981. NMR of membranes. *Progr. NMR Spectrosc.* 14:113-136.

Jähnig, F. 1979. Molecular theory of lipid membrane order. *J. Chem. Phys.* 70:3279-3290.

Janiak, M. J., D. M. Small, and G. G. Shipley. 1976. Nature of the thermal pretransition of synthetic phospholipids: dimyristoyl- and dipalmitoyllecithin. *Biochemistry.* 15:4575-4580.

Jarrell, H. C., J. B. Giziewicz, and I. C. Smith. 1986. Structure and dynamics of a glyceroglycolipid:  $^2\text{H}$  NMR study of head group orientation, ordering and effect on lipid aggregate structure. *Biochemistry.* 25:3950-3957.

Kirk, G. L., and S. M. Gruner. 1985. Lyotropic effects of alkanes and headgroup composition on the  $L_\alpha$ - $H_{II}$  lipid liquid crystal phase transition: hydrocarbon packing versus intrinsic curvature. *J. de Physique.* 46:761-769.

Lewis, B. A., and D. M. Engelman. 1983. Lipid bilayer thickness varies linearly with acyl chain length in fluid phosphatidylcholine vesicles. *J. Mol. Biol.* 166:211-217.

Lis, L. J., M. McAlister, M. Fuller, R. P. Rand, and V. A. Parsegian. 1982. Interactions between neutral phospholipid bilayer membranes. *Biophys. J.* 37:657-666.

Mantsch, H. H., H. Saito, and I. C. P. Smith. 1977. Deuterium magnetic resonance: applications in chemistry, physics and biology. *Progr. NMR Spectrosc.* 11:211-272.

Mely, B., J. Charvolin, and P. Keller. 1975. Disorder of lipid chains as a function of their lateral packing in lyotropic liquid crystals. *Chem. Phys. Lipids.* 15:161-173.

Mouritsen, O. G., and M. Bloom. 1984. Mattress model of lipid-protein interactions in membranes. *Biophys. J.* 46:141-153.

Pauls, K. P., A. L. MacKay, and M. Bloom. 1983. Deuterium nuclear magnetic resonance study of the effects of palmitic acid on dipalmitoyl-phosphatidylcholine bilayers. *Biochemistry.* 22:6101-6109.

Perly, B., I. C. Smith, and H. C. Jarrell. 1985. Effects of the replacement of a double bond by a cyclopropane ring in phosphatidylethanolamines: a  $^2\text{H}$  NMR study of phase transitions and molecular organization. *Biochemistry.* 24:1055-1063.

Rance, M., and R. A. Byrd. 1983. Obtaining high-fidelity spin- $1/2$  powder spectra in anisotropic media: phase-cycled Hahn echo spectroscopy. *J. Magn. Reson.* 52:221-240.

Seelig, J. 1977. Deuterium magnetic resonance. Theory and application to lipid membranes. *Q. Rev. Biophys.* 10:353-418.

Seelig, J., and A. Seelig. 1980. Lipid conformation in model membranes and biological membranes. *Q. Rev. Biophys.* 13:19-61.

Sternin, E. 1985. Data acquisition and processing: a systems approach. *Rev. Sci. Instrum.* 56:2043-2049.

Sternin, E., M. Bloom, and A. L. MacKay. 1983. De-Pake-ing of NMR spectra. *J. Magn. Reson.* 55:274-282.

Thewalt, J. L., A. P. Tullock, and R. S. Cushley. 1986. A deuterium NMR study of labeled *n*-alcohol anesthetics in a model membrane. *Chem. Phys. Lipids.* 39:93-107.

Thewalt, J. L., S. R. Wassal, H. Gorissen, and R. S. Cushley. 1985. Deuterium NMR study of the effect of *n*-alcohol anesthetics on a model membrane system. *Biochim. Biophys. Acta.* 817:355-365.

Tilcock, C. P. S., P. R. Cullis, and S. M. Gruner. 1986. On the validity of  $^{31}\text{P}$  NMR determinations of phospholipid polymorphic phase behavior. *Chem. Phys. Lipids.* 40:47-56.

Yoon, N. M., C. S. Pak, H. C. Brown, S. Krishnamurthy, and T. P. Stocky. 1973. Selective reductions. XIX. The rapid reaction of carboxylic acids with bovine-tetrahydrofuran. A remarkably convenient procedure for the selective conversion of carboxylic acids to the corresponding alcohols in the presence of other functional groups. *J. Org. Chem.* 38:2786-2792.